Available online at www.sciencedirect.com

ScienceDirect

Physics Procedia 14 (2011) 231–234

Physics Procedia

9th International Conference on Nano-Molecular Electronics

Thick polymer blend organic solar cells fabricated by slow drying

Hiroyuki Ogo[a]*, Toshihiro Yamanari[a], Tetsuya Taima[a,b], Jun Sakai[c], Jun Tsukamoto[d], and Yuji Yoshida[a]

[a]*Research Center for Photovoltaics, National Institute of Advanced Industrial Science and Technology (AIST), AIST Tsukuba Central 5, 1-1-1 Higashi, Tsukuba 305-8565, Japan*

[b]*JST-PRESTO, Japan Science and Technology Agency (JST), 4-1-8 Honcho Kawaguchi, Saitama 332-0012, Japan*

[c]*Advanced Technologies Development Laboratory, Panasonic Electric Works, Ltd., 1048 Kadoma, Osaka 571-8686, Japan*

[d]*Electronic and Imaging Materials Research Laboratories, Toray Industries, Inc., 3-2-1 Sonoyama, Ohtsu 520-0842, Japan*

Abstract

Organic solar cells (OSCs) were generally fabricated by two types of deposition method, namely, dry and wet. Many OSCs use very thin films that cannot fully absorb light. Thick film deposition for OSCs has numerous benefits, such as highly efficient harnessing of solar light and low leakage. Thick film fabrication for polymer blend organic solar cells by the wet deposition method was investigated. OSCs were fabricated by spin coating and slow drying using P3HT and bis[60]PCBM in a solvent, respectively. Two-dimensional (2D)-mapping images of the photocurrent of the cells were measured by a laser-beam-induced current method. A low-current density area was not found in all the cells. As a result, we succeeded in fabricating OSCs with a power conversion efficiency of more than 4 % by slow drying.

Keywords: organic solar cell; polymer blend film; thick film; wet-process

1. Introduction

Recently, organic solar cells (OSCs) have received considerable attention as a next-generation energy source. OSCs, which have been studied by many researchers, are low cost, light and flexibly [1-3]. Dry and wet deposition methods are suitable for organic film deposition. For the wet deposition method, OSCs were fabricated in a remarkably simple way. Furthermore, the wet deposition method can be applied to a roll-to-roll process that has many advantages, such as large-scale device area, low processing cost, and high throughput [4,5]. In recent years, a cell with high power conversion efficiency (PCE) has been reported [6-9]. OSCs generally use thin films, because the organic semiconductor used has poor charge carrier transport. In many cases, OSCs use very thin films that cannot fully absorb sunlight. To use solar light more efficiently, the thicknesses of OSCs should be larger than 100

* Corresponding author. Tel.:+81-29-861-6246; fax:+81-29-861-6232.
E-mail address:hiro-ogou@aist.go.jp.

1875-3892 © 2011 Published by Elsevier Ltd. Open access under CC BY-NC-ND license.
doi:10.1016/j.phpro.2011.05.047

nm, which is generally used in the case of thin films. In addition, to industrialize OSCs, thick film deposition with numerous benefits, such as efficient harnessing of solar light and low leakage, should be carried out. Thick film OSCs were reported to be fabricated by the vacuum deposition method developed by Suemori et al. using a low-molecular-weight device [10]. In this work, thick film fabrication for mixing regioregular poly(3-hexylthiophene) (P3HT, Merck) used as a *p*-type semiconductor and [6,6] diphenyl C_{62} bis (butyric acid methyl ester) (bis[60]PCBM, Solenne) used as an *n*-type semiconductor organic film by the wet deposition method was studied.

2. Experimental

Glass substrates with 10 Ω/sq indium-tin oxide (ITO) were used. First, to clean their surfaces, the ITO substrates were exposed to oxygen plasma. OSCs were fabricated by sandwiching a polymer blend organic film between an ITO anode and an aluminum (Al) cathode. Polymer blend organic films were prepared by two types of wet deposition method: the spin coating method whose speed ranged from 300 to 3000 revolutions per minute (rpm) and the slow drying method that involves more natural drying after operation from 300 to 3000 rpm for 3 seconds by spin coating. An approximately 30-nm-thick PEDOT:PSS layer (Baytron P VP. Al 4083, H.C. Starck Ltd.) used as a hole transport layer was deposited on an ITO substrate by spin coating (3000 rpm, 180 s), and then the substrate was dried on a hot plate (135 °C, 10 min) in air. P3HT (10 mg) and bis[60]PCBM (15 mg) were dissolved in 1 ml of chlorobenzene (CB) and 1 ml of mixed solvent composed of chloroform (CF) and *o*-dichlorobenzene (DCB) (8:2), respectively. In both wet deposition methods, film thicknesses were controlled to be approximately 100 nm and 300 nm. Subsequently, Al was vacuum-deposited on the organic layer with a thickness of about 120 nm. The effective areas of the cells were 1.21 cm^2. For all devices, thermal annealing treatments were carried out in the glove box filled with nitrogen. The surface morphology of organic films was observed by tapping-mode atomic force microscopy (AFM, SII E-sweep NanoNavi).

The solar cell characteristics were measured under illumination using an Air Mass 1.5 Global (AM1.5G) what light intensity was calibrated to 100 mW/cm^2 by using a reference cell for a-Si solar cells. Current density-voltage (*J*-*V*) characteristics were measured using a Keithley 2400 source measurement unit. The photocurrent distribution due to defects was studied. Two-dimensional (2D)-mapping images of the photocurrent of the cells were measured using a laboratory-built laser-beam-induced current (LBIC)-measuring system [11].

3. Results and discussion

3.1. Solar cell characteristics

Table 1 shows the characteristics of the solar cells fabricated by two different methods. Thin film OSCs showed high fill factor (FF) and low current density (*J*sc). The characteristics of thick film OSCs fabricated by spin coating showed low FF and *J*sc. On the other hand, the characteristics of thick film OSCs fabricated by slow drying in the mixed solvent showed high FF and *J*sc. As a result, we succeeded in fabricating OSCs with a power conversion

Table 1. Characteristics of P3HT:bis[60]PCBM solar cell.

Deposition method	Thickness	Solvent	PCE (%)	*J*sc (mA/cm^2)	*V*oc (V)	FF
Spin coating	~ 100 nm	CB	3.1	6.78	0.72	0.63
Spin coating	~ 300 nm	CB	2.0	6.63	0.69	0.43
Spin coating	~ 100 nm	CF/*o*-DCB	2.0	6.12	0.59	0.55
Spin coating	~ 300 nm	CF/*o*-DCB	2.8	8.02	0.67	0.52
Slow-drying coating	~ 100 nm	CB	2.5	5.94	0.71	0.60
Slow-drying coating	~ 300 nm	CB	1.6	6.29	0.64	0.39
Slow-drying coating	~ 100 nm	CF/*o*-DCB	2.9	6.63	0.68	0.64
Slow-drying coating	~ 300 nm	CF/*o*-DCB	4.0	8.66	0.73	0.63

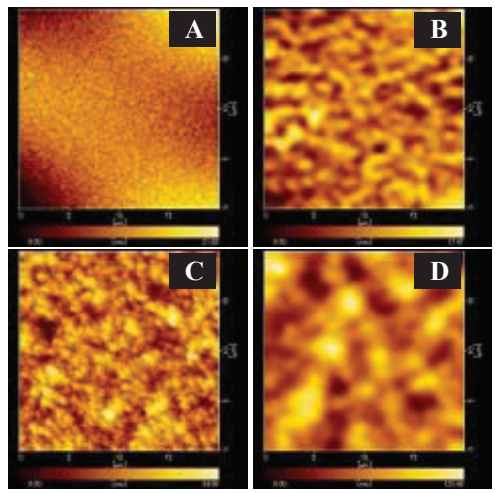

Figure 1 AFM images of organic films; A; spin coating (~100 nm, CB); B: spin coating (~300 nm, CB); C: slow drying (~100 nm, CF/DCB); D: slow drying (~300 nm, CF/DCB). Image dimensions: 20 x 20 μm^2.

efficiency of more than 4% by slow drying.

3.2. AFM surface morphology analysis

Figure 1 shows AFM images of organic films fabricated by the two types of deposition method. The following are the values of root mean square (RMS) roughness: spin coating (~100 nm, CB): 1.17 nm; spin coating (~300 nm, CB): 2.78 nm; slow drying (~100 nm, CF/DCB): 13.4 nm; slow drying (~300 nm, CF/DCB): 19.3 nm. The grain size of thick films increased to more than that of thin films. Additionally, the grain size of the films fabricated by slow drying increased greater than that of the films fabricated by spin coating. From these results, it is considered

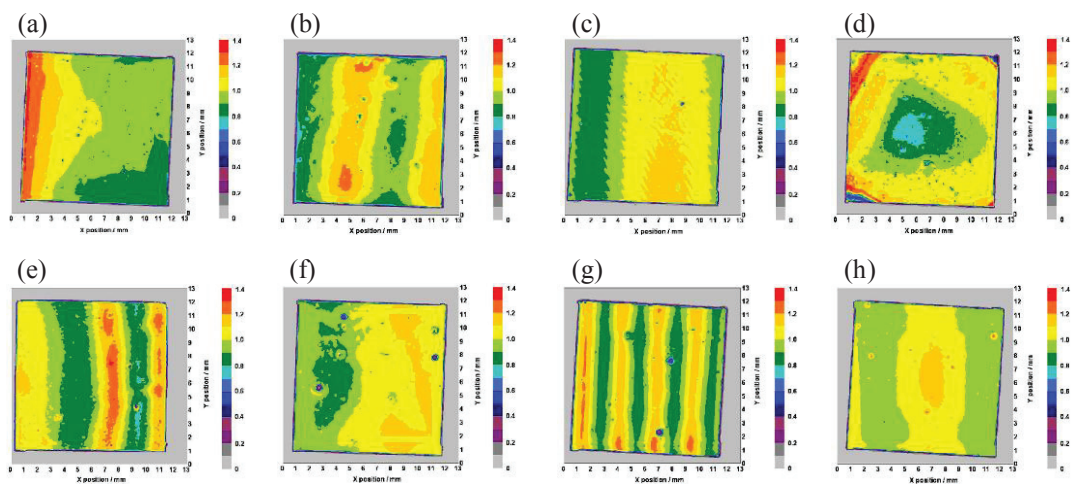

Figure 2 LBIC mapping images of OSCs: (a): spin coating (~100 nm, CB); (b): spin coating (~300 nm, CB); (c): slow drying (~100 nm, CB); (d): slow drying (~300 nm, CB); (e): spin coating (~100 nm, CF/DCB); (f): spin coating (~300 nm, CF/DCB); (g): slow drying (~100 nm, CF/DCB); (h): slow drying (~300 nm, CF/DCB). Contrasts show photocurrent differences.

that when the film deposition methods used are different, the surface morphologies of films are significantly different. It is also considered that the drying and volatilization rates the solvent contribute to grain growth. The high solar cell characteristic of the thick film cell indicates that the transport of carriers was improved by the marked increase in grain size.

3.3. Photocurrent 2D mapping by LBIC measurement

Figure 2 shows the 2D-mapping images of the photocurrent of the cells for various fabrication conditions measured by the LBIC method. In the active area, the lowest photocurrent is higher than 0.6. Thus, the difference between the highest and lowest currents is less than 0.8, which indicates a uniform photocurrent distribution in all the cells. In addition, the LBIC image of the cell fabricated by slow drying (~300 nm, CF/DCB) exhibits a more uniform photocurrent distribution. As a result, the cell fabricated by slow drying (~300 nm, CF/DCB) has high *J*sc.

4. Conclusions

We have fabricated polymer blend OSCs by two types of wet deposition method, namely, spin coating and slow drying methods. Thick film deposition for OSCs was achieved. Thick films fabricated by slow drying had a higher PCE than those fabricated by conventional spin coating. The grain size of the slow-drying-deposited films was larger than that of conventional-spin-coating-deposited films. In the active area, the difference between the highest and lowest currents was less than 0.8, which indicates a uniform photocurrent distribution in all the cells. Finally, we succeeded in fabricating OSCs with a PCE of more than 4 % by the slow drying.

Acknowledgements

This work was supported by the Incorporated Administrative Agency New Energy and Industrial Technology Development Organization (NEDO).

Reference

[1] B. J. Lee, H. J. Kim, W.-I. Jeong, J.-J. Kim, *Sol. Energy Mater. Sol. Cells* **94** (2010) 542-546
[2] S.-S. Kim, S.-I. Na, S.-J. Kang, D.-Y. Kim, *Sol. Energy Mater. Sol. Cells* **94** (2010) 171-175
[3] X. Guo, F. Liu, B. Mehg, Z. Xie, L. Wang, *Org. Electron.* **11** (2010) 1230-1233
[4] F. C. Krebs, *Sol. Energy Mater. Sol. Cells* **93** (2009) 465-475
[5] F. C. Krebs, *Org. Electron.* **10** (2009) 761-768
[6] D. Cheyns, B. P. Rand, P. Heremans, *Appl. Phys. Lett.* **97** (2010) 033301
[7] Y. Liang, Z. Xu, J. Xia, S-T. Tsai, Y. Wu, G. Li, C. Ray, L. Yu, *Adv. Mater.* **19** (2007) 3973
[8] D. Kitazawa, N. Watanabe, S. Yamamoto, J. Tsukamoto, *Appl. Phys. Lett.* **95** (2009) 053701
[9] J. Sakai, K. Kawano, T. Yamanari, T. Taima, Y. Yuji, A. Fujii, M. Ozaki, *Sol. Energy Mater. Sol. Cells* **94** (2010) 376-380
[10] K. Suemori, T. Miyata, M. Yokoyama, M. Hiramoto, *Appl. Phys. Lett.* **86** (2005) 063509
[11] T. Yamanari, T. Taima, J. Sakai, J. Tshukamoto, Y. Yoshida, *Jpn. J. Appl. Phys.* **49** (2010) 01AC02